ISRAEL JOURNAL OF TECHNOLOGY, Vol. 8, No. 1–2 1970, pp. 73–85
Proc. XII Israel Ann. Conf. AVIATION and ASTRONAUTICS, March 1970

The Electrostatic Probe: Some Applications to Hypersonic Flow Diagnostics

S. LEDERMAN*, M. H. BLOOM** AND J. AVIDOR***

Polytechnic Institute of Brooklyn, Farmingdale, New York, U.S.A.

Received November 11, 1969

ABSTRACT

Results of an experimental investigation of the applicability of electrostatic cylindrical probes for flow field diagnostics are presented. An experimental extension of the formulation of the free-molecular collisionless operation of cylindrical probes into the transitional and continuum regime is provided. It is shown that the power law valid for the free-molecular collisionless regime with $0.1 < r_p/\lambda_D < 3$ is applicable in the transitional and continuum regime where r_p/λ_D may exceed 3. Experimental results obtained in the wake of several models, using the electrostatic probe technique, are compared with results obtained by other means. These results confirm the basic principle and soundness of this technique.

NOTATION

B — bluntness ratio $= \frac{R_n}{R_b}$
d — probe diameter
e — electron charge
J — current density
k — Boltzmann's constant
l — probe length
m — mass of particle
N — particle number density
Q_0 — quality factor of cavity without plasma
Q — quality factor of cavity with plasma
R_p, r_p — probe radius
R_n — nose radius
R_b — base radius
T — temperature
V — random ion velocity $= \left(\frac{8kT_e}{\pi m_i}\right)^{\frac{1}{2}}$
x_p — dimensionless normalized probe potential $= \frac{e(V-V_\infty)}{kT}$
x — axial coordinate
y — radial coordinate
α_p — dimensionless normalized probe current density
ε_0 — dielectric constant
λ — mean free path
λ_D — Debye shielding distance $= \left(\frac{\varepsilon_0 kT_e}{N_e e^2}\right)^{\frac{1}{2}}$
ρ — density
ω_0 — resonant frequency of cavity
ω_p — plasma frequency $= \left(\frac{N_e e^2}{\varepsilon_0 m_e}\right)^{\frac{1}{2}}$
ν — electron-neutral collision frequency

SUBSCRIPTS

e — electron
i — ion
n — neutral
∞ — free stream

I. INTRODUCTION

Recent developments in hypersonic simulation resulted in a greatly increased number of physical and chemical phenomena which may be investigated in ground based facilities. These investigations range from shock formation to shock shape, from flow field tracing to field (flow) visualisation, from the degree of ionization to the ionozation reaction constants, from shock compression to wake expansion or from communications to observation and recognition with all the pertinent interactions. It is quite irrelevant if some of the phenomena under investigation are or are not directly associated with atmospheric reentry.

* Associate Professor of Aerospace Engineering.
** Director of Gas Dynamics Research.
*** Formerly J. Oberndoerfer; Research Associate.

BLANK PAGE

The results of these investigations have, in any case, greatly contributed to the understanding of the nature of atmospheric reentry as well as of the basic phenomena associated with it. Simultaneously with the expanded scope of this research, a great number of scientists were involved in developing the necessary diagnostic instrumentation for those facilities. Among a variety of diagnostic instruments the electrostatic probe became the center of a great deal of attention (*Bernstein and Rabinowitz*, 1959; *de Leeuw*, 1963; *Graf*, 1965; *Laframboise*, 1966; *Sonin*, 1966; *Su and Lam*, 1963). The unusual interest in this instrument, which is one of the oldest known plasma diagnostic instruments (*Langmuir and Mott-Smith*, 1926), must be traced to its simplicity, size, and extraordinarily wide dynamic range. Electron densities of 10^4 to 10^{15} el/cm^3 are reported to have been measured by probes. There is no other simple instrument of such an enormous dynamic range. The external circuitry necessary for the operation of these instruments is again extremely simple. A resistor battery or D.C. power supply, and recording device, is all that is necessary to perform a measurement. The frequency response of an electrostatic probe is sufficiently high (typically 10^6 sec^{-1}) for most practical measurements in a hypersonic simulation facility. These positive qualities of an electrostatic probe are, however, overshadowed to a certain extent by the difficulties in relating the collected currents to the actual number densities of a given plasma. Since its inception, scores of scientific papers have been published dealing with this problem. There is, however, no general unified theory covering the whole range of probe operation in an arbitrary plasma, which would afford the experimentalist a simple method of obtaining quantitative results from the collected probe currents. There are certain regimes of plasmas for which sound theoretical, as well as experimental, background exists to warrant the application of the electrostatic probe to some fluid dynamic diagnostics. These pertain in particular to diagnostics of flows in hypersonic shock tunnel facilities. In this paper, after a discussion of some of the results of theoretical considerations for ion collecting probes, their range of applicability, and their limitations, experimental evidence is presented substantiating in part some of the theoretical predictions of the free molecular collisionless theory and modifying and extending the range of applicability of ion collecting probes into the orbit motion limited regime as well as into the transitional and continuum regime. These results are subsequently used to determine the pointwise electron density distribution in in the near wake of some blunt and sharp-nosed cone models, as well as the shock shape. It is shown that under certain conditions, the electron densities can be related to the neutral density distribution in most of the flow fields under consideration. The range of applicability of this technique is discussed and the limitations are pointed out. A comparison with results obtained, using the electron beam method under similar test conditions (*Munz and Zempel*, 1963) confirms that this simple electrostatic probe method permits one to obtain at least qualitative flow field patterns.

II. REVIEW AND EXTENSION OF THE ELECTROSTATIC PROBE THEORY

As pointed out in the Introduction, there is no unified theory which will permit one to obtain exact number densities from the collected currents on probes, irrespective of the plasma regime. In the course of development of the electrostatic probe theories and techniques, it became clear that charged particle collection by probes is not only affected by the probe potentials, the number densities of the plasma and the thermal velocities of the collected species, but also by a large number of other interacting parameters. Among these are the temperature ratio of the electrons and ions, the ratio of the Debye length to the probe radius, the mass motion relative to the probe versus the mean random speed of the particles, and the probe dimensions relative to the mean free path of the different species in the given plasma. In view of these parameters the plasmas dealt with in practice, can be divided into two groups: First the stationary plasmas, where there is no mass motion with respect to the probes (like in a discharge), and second, directed motion of the plasma as in a plasma jet or an ionized hypersonic flow. These groups can in turn be subdivided into several operating regimes: First, the collisionless free molecular regime where the mean free path of the species involved are large compared to the radii of the collecting probes.

Second, the transitional regime, where some of the mean free paths are of the same magnitude as the radii of the collecting probes, and last, the continuum regime where all the mean free paths of the species are small compared to the probe radii. It should be noted here that the above subdivision of the plasma operating regimes is only a very rough one. It is, however, sufficient for the purposes of this investigation. Of the above regimes, the free molecular collosionless regime in a stationary plasma received the most attention. The work of Laframboise, dealing with this regime, based on the theory of Bernstein and Rabinowitz for monoenergetic particle collection, represents a very important milestone in the free molecular collisionless probe theory. Based on this work it is possible to obtain the electron density from the collected ion currents in a free molecular collisionless plasma at rest. In a flowing plasma these results are applicable provided long cylindrical probes with their axis oriented in the flow direction are used. Since this work is concerned with the application of the probes to flow field diagnostics, only the behavior of cylindrical probes is investigated.

For cylindrical probes the collected ion saturation current can formally be expressed in the following way:

$$J_i = \frac{N_i e v}{4} \alpha_p \left(\kappa_p, \frac{r_p}{\lambda_D}, \frac{T_i}{T_e} \right) \tag{1}$$

which represents the random current density modified by a factor which is a complex function of several interacting parameters. This current factor was calculated for a range of parameters by Laframboise (1966), for both cylindrical and spherical probes, for a plasma at rest. The range of applicability of the Laframboise theory is, however, very limited. The requirement of the free molecular conditions on the one hand and the limitations imposed by the r_p/λ_D requirements on the other, imposes restrictions on the number densities and degree of ionization of the plasma under investigation. In the case of a very low degree of ionization as, for example, in a plasma with $\lambda_{n-n} = \lambda_{i-n} \approx 2$ mm with a number density corresponding to a λ_D of 5.8 mm [$n = 10^6$ $T_e = 3000°K$], the requirement of free molecular operation, limits the probe diameter to less than 2 mm. This results in an $r_p/\lambda_D < 1$, which is outside the range of applicability of the Laframboise theory, To extend the applicability of the probes into this range, an experimental investigation was undertaken by Lederman et al. (1968). They have shown that under the conditions encountered in their hypersonic shock tunnel facility, the number density of the ionized particles can be determined using the formal expression of Laframboise without the restriction to $r_p/\lambda_D > 3$. They obtained experimentally the values of the nondimensional normalized current α_p for r_p/λ_D from 3 to less than 0.1. They furthermore found a relation between current density and the fineness ratio, thus permitting the use of very small probes to achieve better spacial resolution. These results are shown in Figs. 1 and 2 for a fixed probe potential.

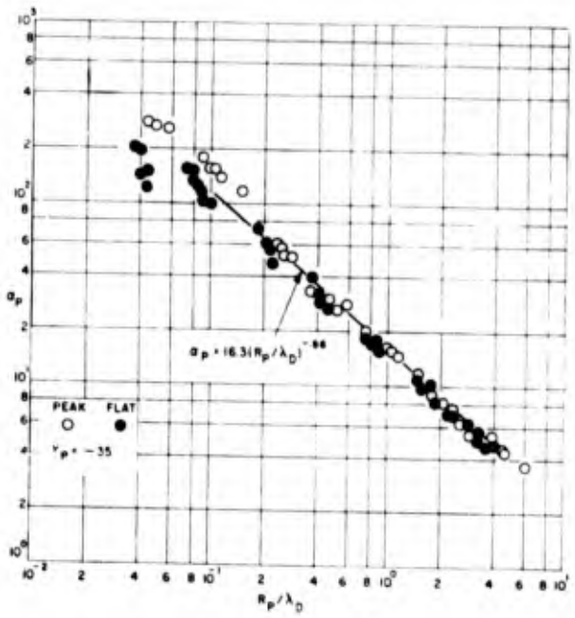

Fig. 1. Normalized nondimensional ion current as a function of the ratio of probe radius to Debye shielding distance in the free molecular regime.

As indicated above, the transitiona !and continuum regimes of probe operation are less well-founded theoretically as well as experimentally than the free molecular collisionless regime. This may be attributed to a number of reasons, the main reasons being the extremely complicated behavior of the ionized particles. The appearance of collisions increases the complexity of the equations of motion to such an extent that an analytical solution becomes extremely difficult. This is particularly true for the transitional regime, where neither the free molecular nor the con-

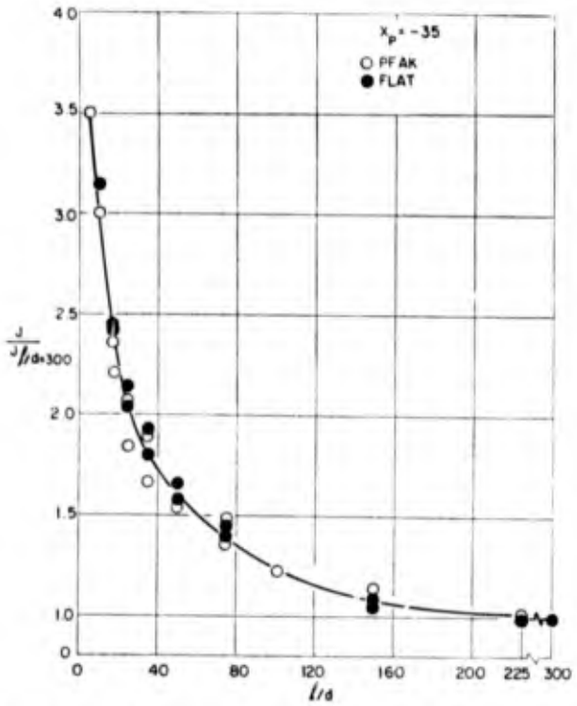

Fig. 2. Nondimensional current density as a function of the probe length-to-diameter ratio.

tinuum theories apply. In view of the above, an attempt was made in this work to obtain experimentally a correlation between the probe collected ion current density and the corresponding electron number density in a regime where some of the free molecular collisionless probe theory conditions are violated. As shown previously (*Lederman* et al., 1968), the formal equation derived by Laframboise (Eq. 1) remains valid in the regime where all requirements of the free molecular collisionless theory are satisfied except the requirement that $r_p/\lambda_D > 3$, and l/d be infinite. This formalism was preserved by obtaining experimentally the α_p factor as a function of r_p/λ_D for finite l/d ratios, and the dependence of the collected current density on the magnitude of l/d as indicated in Figs. 1 and 2. To obtain the same kind of data for the transitional regime, it was decided to utilize the flow in the nozzle of the shock tunnel as the test medium. Here the mean free paths of the particles could be continuously varied maintaining the velocity almost constant. The slight changes in the electron and ion temperatures as one moves from the test section into the nozzle up to about 100 cm from the throat (length of the nozzle 440 cm) can be neglected, particularly since T_i/T_e in any case remains much smaller than 1 and the random ion velocity as defined varies only as the square root of the electron temperature T_e. Following the same procedure as in Lederman, (1963), a rake containing four rows of eight probes each was constructed. One row contained eight probes of the same diameter with a variable l/d ratio; the second row contained eight probes of the same size to check on the uniformity of the flow; the last two rows contained two sets of probes of the same l/d ratio but of variable diameter ranging from 0.00254 cm to 0.2032 cm. These probes not only provided a variation of r_p/λ_D but also provided a link between the free molecular and transitional or continuum regimes. This is evident from Table I where the mean free paths are tabulated. As can be seen from this table, in the test section at $x = 440$ all probes have dimensions smaller than the mean free paths. As the rake is moved upstream the flow remains free molecular for some probes, transitional for others, and becomes continuous — as far as λ_{n-n} is concerned — for the remainder. To correlate the collected ion current density to the corresponding electron number density, a microcave resonant cavity was used. The electron number density obtained using the microwcave resonant cavity technique was used not only to compute the corresponding nondimensional current factor α_p in the transitional and continuum regime, but also to compare the electron number density obtained from the Laframboise theory in the range of applicability of the same.

III. THE MICROWAVE RESONANT CAVITY

The resonant cavity method of plasma diagnostics exploits the change in the parameters of a resonant cavity which may be completely or partially filled with a plasma. When a microwave resonant cavity is filled with a plasma, both its resonant frequency and its quality factor are changed. By measuring the shift in resonant frequency and the change in Q, it is possible to determine the plasma parameters, such as the electron number density and the electron neutral collision frequency. A schematic drawing of such a cavity is shown in Fig. 3. It consists of a short metal cylinder, through the center of which a thin walled 2.54 cm I.D. teflon tube is inserted. This tube constitutes the flow region of the ionized gas through the cavity and provides the interaction region of the

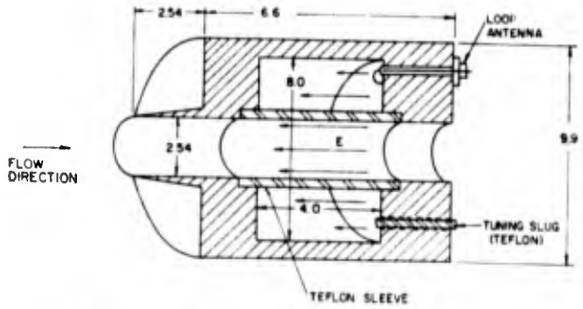

Fig. 3. Schematic diagram of the TM_{010} cavity.

ionized gas with the applied electromagnetic field in the cavity. The dielectric tube is preceded by a sharp edged cylinder of the same I.D. The length of this cylinder is designed to be larger than the stand-off distance of the shock formed over the cavity structure, and minimizes the disturbance of the entering flow. The cavity is operated in the TM_{101} mode. Since the electric field is essentially parallel to the axis of the cavity with the greatest concentration in the center portion, maximum interaction of the field with the ionized gas is insured. The operation of this kind of a cavity for plasma diagnostics is well-covered in the literature (*Bloom and Lederman*, 1967; *Heald and Wharton*, 1965; *Lederman* et al., 1967; *Lederman* et al., 1964). The basic equations governing the operation of this type of a cavity are:

$$\frac{\Delta\omega}{\omega_0} = K\frac{\omega_p^2}{\omega_0^2}\frac{1}{1+\left(\frac{\nu}{\omega_0}\right)^2} \tag{2}$$

$$\frac{1}{Q}-\frac{1}{Q_0} = \Delta\left(\frac{1}{Q}\right) = 2K\frac{\omega_p^2}{\omega_0^2}\frac{\frac{\nu}{\omega_0}}{1+\left(\frac{\nu}{\omega_0}\right)^2} = \frac{2\Delta\omega}{\omega_0}\frac{\nu}{\omega_0} \tag{3}$$

When the collision frequency is small $\nu \ll \omega_0$, as in the present cases where ν/ω_0 is of the order of 0.01, the above equations reduce to

$$\frac{\Delta\omega}{\omega_0} = K\frac{\omega_p^2}{\omega_0^2}$$

This equation permits a calibration procedure to determine the configuration constant K. The calibration procedure consists of filling the tube of the cavity with a dielectric of known dielectric constant and noting the shift in the resonant frequency of the cavity. From the last equation the electron density of a collisionless plasma is computed yielding the same frequency shift as the dielectric, and from the equivalency of the absolute value of the two dielectrics, the constant K is determined. Thus, a knowledge of K and measurement of the resonant frequency shift permits the determination of the electron number density N_e. The value of N_e thus measured is the average value of the electron number density which can be found at a given time in the cavity. The method is thus insensitive to nonuniformities of the electron density distribution in the cavity. For the cavities utilized in this investigation, a calibration curve showing the resonant frequency shift vs. the electron number density is shown in Fig. 4.

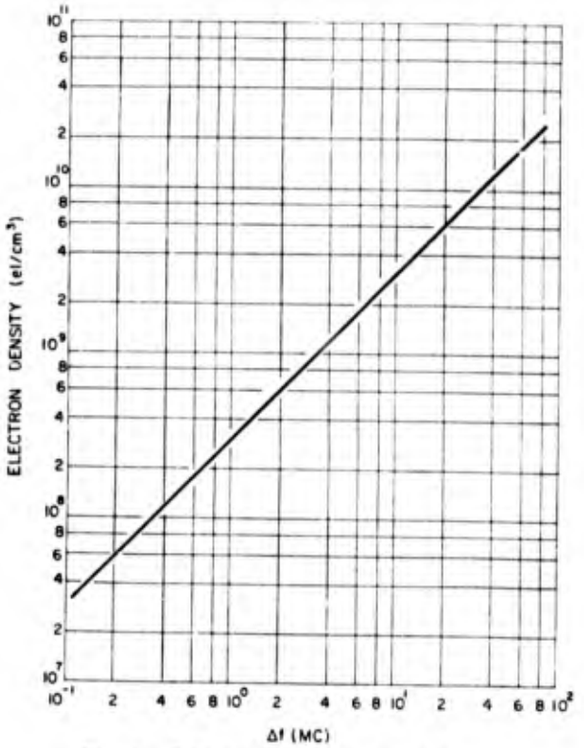

Fig. 4. Calibration of the S-band cavity.

It should be pointed out that this cavity can be operated as an absorption or transmission cavity. In this investigation the cavity was operated as a transmission cavity. The experimental procedure is as follows: The applied frequency to the cavity is preset by a given Δf corresponding to a fixed number density. In case the number density is higher than the preset value, two resonant peaks occur; if the number density is lower than the preset frequency shift, no resonant peak occurs.

IV. EXPERIMENTAL APPARATUS

The apparatus used in this research program was the hypersonic shock tunnel of the Polytechnic Institute of Brooklyn, located at the Graduate Center in Farmingdale. A detailed description of the facility and its performance capabilities were described previously (*Visich* et al., 1965; *Bloom and Lederman*, 1967). In order to maintain the test section under vacuum between tests, a slide valve was inserted in in the primary nozzle. This slide valve permits the change of diaphragms at the throat of the primary nozzle and the opening of the shock actuated valve without the necessity of pressurizing the test section. This valve thus permits the test section models and probes to remain under vacuum and thus free from contamination by the atmospheric air. The operating initial conditions of the shock tunnel were fixed throughout this investigation. With an initial driven pressure of 38 mm Hg air, and a driver pressure of 1800 psi helium, a shock Mach number of about 7 was obtained. This resulted in a pressure of about 23 atmospheres and a temperature of about 3800°K behind the reflected shock. After expansion, the test chamber conditions were: Mach number $\sim$ 18, density—2.2×10^{-8} *gr/cm*^{3}, mean free path about 0.6 cm. The free stream electron density was measured and found to be between $2\text{–}5\times10^8$ el/cm^3. When compared with the ambient neutral density of about 5×10^{14} p/cm^3, this results in about one ionized particle in one million and can, therefore, for all practical purposes, be neglected as far as its influence on the flow field is concerned. It can, however, in the context outlined previously (*Lederman* et al, 1969*b*), be considered as a convenient tracer of the neutral density variation in nondiffusive regions since the flow is chemically frozen. The uniformity of the flow in the test section was determined and found to occupy a central core of the test section of about 24 inches (*Bloom and Lederman* 1967). This uniform flow region was found to be of sufficient magnitude to accommodate reasonably sized models with an adequate number of instruments. The models tested were a 10° half angle cone of 10.16 cm base diameter at 0° and 10° angles of attack, a 10° half angle cone of 15.24 cm base diameter of 0.333 and 0.666 bluntness ratio at 0° angle of attack, and an Apollo Command Module type model. The models were suspended in the center of the test section by 0.5 mm wires. Flow field interference resulting from these supports could be considered negligibly small, since their dimensions were considerably less than the mean free path of the test section gas flow. Two kinds of rakes of electrostatic probes were used in this work. The first rake consisted actually of four rows of eight probes each spaced 1.27 cm apart. This rake was used to determine the probe characteristics. The probe arrangement in these tests was similar to the one followed elsewhere (*Lederman* et al., 1968). The other rake used to obtain the data in the wake of the models was designed with the flow field in mind (*Lederman* et al., 1969*b*). The The test section configuration is shown schematically in Fig. 5.

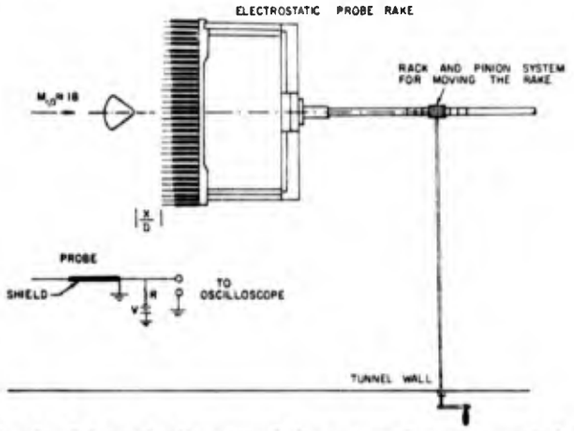

Fig. 5. Schematic diagram of the test configuration and the electrostatic probe circuit.

V. EXPERIMENTAL RESULTS

Two series of tests were conducted. One series was concerned with determination of the electrostatic probe behavior, the other with the application of the probes to flow field diagnostics. In the former one, as indicated above, a rake containing four rows of eight probes each was mounted on a movable sting. Since the probes were of the plug-in type, their arrangement could be easily changed. In each test the rake contained a number of probes which were of a variable diameter and the same *l*/*d* ratio, a number of probes of the same diameter and variable *l*/*d* ratio and a number of probes of the same diameter and the same *l*/*d* ratio. The latter group of probes was used to check on the uniformity of the flow. Two microwave resonant cavities mounted on the same sting and aligned with the probe rakes to correspond approximately to the same axial position in the nozzle represented

the test configuration. This sting was moved stepwise from the test section into the nozzle. In this configuration the probes were always aligned with the flow direction. A number of tests were run under the same initial test conditions, at different stations in the nozzle. The electron densities as obtained by the cavities and the ion currents of each probe were recorded. It should be noted that the potentials of the probes were all kept at the same constant value, negative with respect to ground, for ion collection.

In Fig. 6, a few samples of the oscilloscope traces of the collected ion currents are presented. These correspond to traces obtained by the same probe at different stations in the nozzle. As may be surmised, they correspond to different regimes of probe operation. Not only are the mean free paths decreasing as the probe rake is moved upstream, but also the Debye shielding distance λ_D is decreasing. It is noticed that as the mean free path and the Debye shielding distance is decreasing, the initial peak on the probe response disappears. The data were reduced using the peaks and the flats of the response traces. The number densities obtained by the microwave resonant cavity measurements were compared to the nonequilibrium calculations of the nozzle flow. Figure 7 shows the experimental as well as the

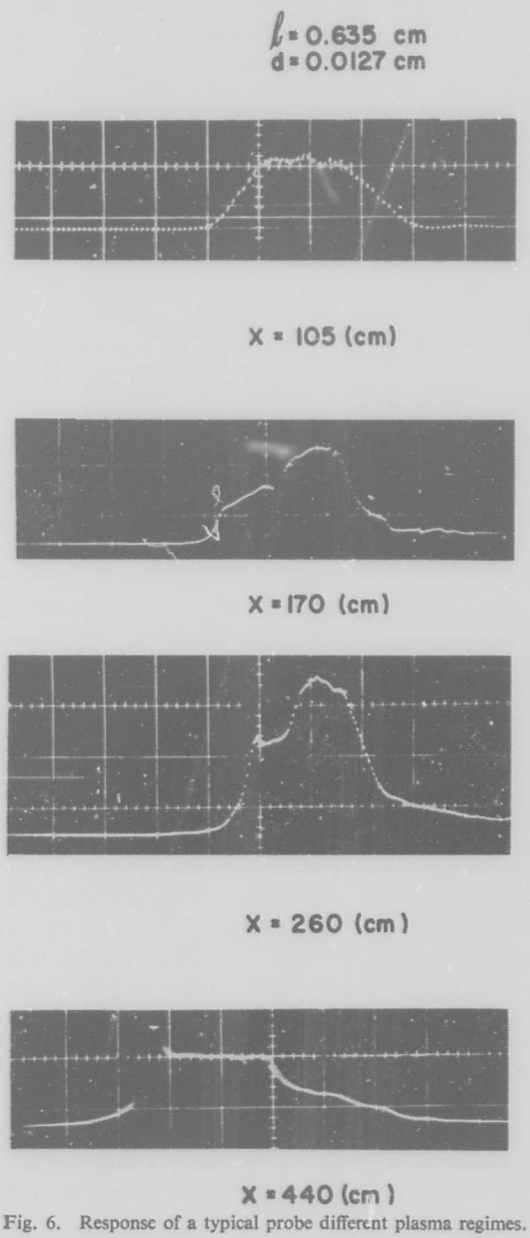

Fig. 6. Response of a typical probe different plasma regimes.

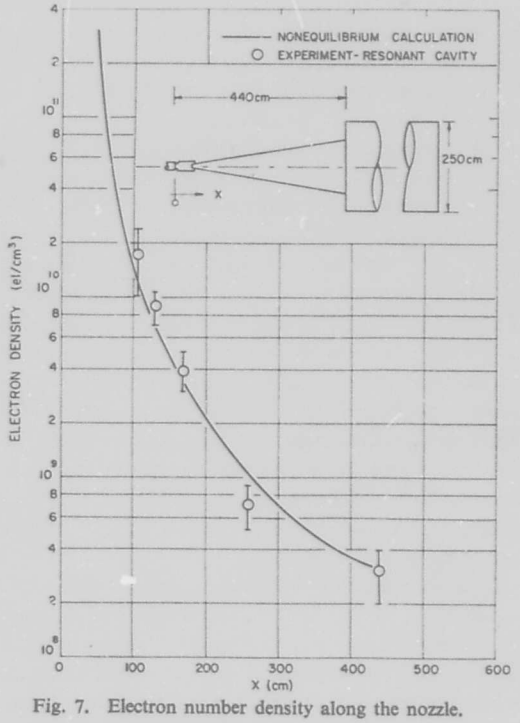

Fig. 7. Electron number density along the nozzle.

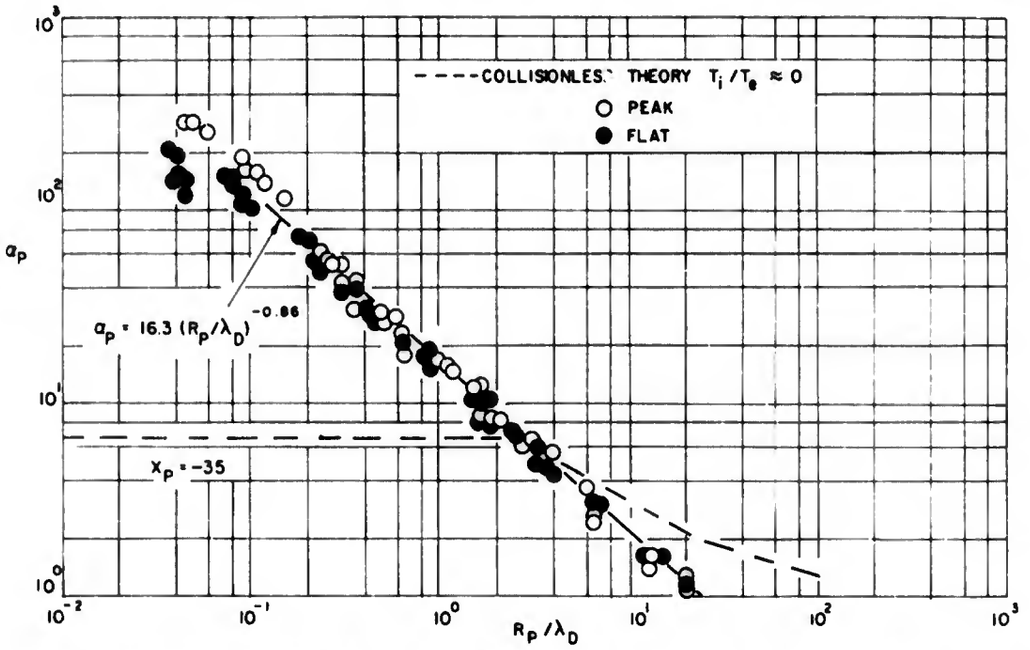

Fig. 8. Normalized nondimensional ion current as a function of the ratio of the probe radius to the Debye shielding distance extended into transitional and continuum regime.

theoretical results. The scatter of the experimental points is within the accuracy one can expect from this type of a resonant cavity in this flow field. These data were obtained by a boundary layer correction of the raw data. The strong viscous-inviscid interaction parameter was taken into account. Since, for most test stations, the smallest diameter probes were still in the free molecular regime, the electron number density was computed utilizing the corresponding collected current density and the data of Figs. 1 and 2. The agreement with the microwave cavity data was remarkable. In view of this and the data in Fig. 7, the electron number densities obtained by the microwave cavity technique at each axial station in the nozzle was used to compute the r_p/λ_D parameter for each probe and the corresponding α_p to satisfy the formal relation of Eq. (1). The results of these tests are shown in Fig. 8, where the parameter α_p as a function of r_p/λ_D is plotted.

In the second series the models were kept stationary, suspended in the test section, and a rake with 32 probes of the same diameter and length-to-diameter ratio was moved from a position of $x/D = 0.25$ to 6. In each station several tests were run and the data reduced utilizing the experimental results obtained previously, where the probe characteristics were determined.

As indicated above, several models of different bluntness ratios and a model of the Apollo Command Module have been tested in the uniform flow field of the test section of the hypersonic shock tunnel. All the tests were conducted in the flow resulting from the same initial conditions in the driven and driver section of the tunnel. A rake of electrostatic probes was used as the only diagnostic tool. Sample oscilloscope traces as obtained in these tests are shown in Fig. 9. These traces arranged from top to bottom correspond to the probes from the centerline behind the model out into the free stream. A sample of the reduced electron densities normalised to the free stream electron density in the near wake behind the 10.16 cm diameter cone of 0° angle of attack at $x/D = 0.25$ is shown in Fig. 10. The data presented here include both the peak and flat portions of the response, both normalized to their respective portion in the free stream. As can be seen here and as shown in Lederman et al. (1969*a*;*b*), the qualitative behavior of the electron density profile can be obtained using either.

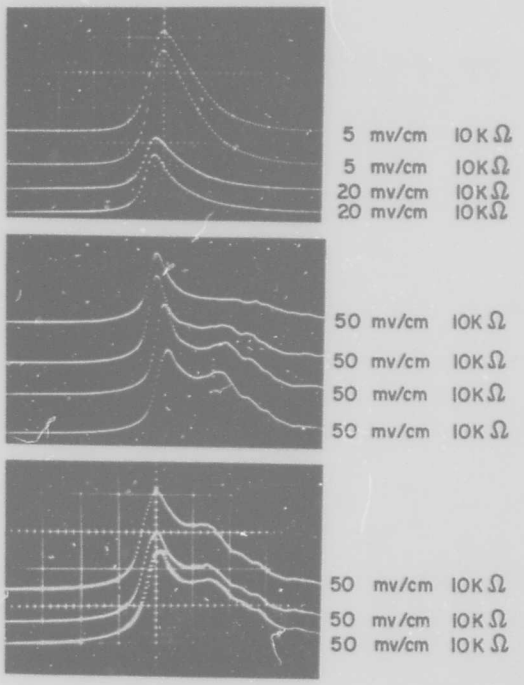

Fig. 9. Response of probes in the wake. Top to bottom represent centerline to free stream responses.

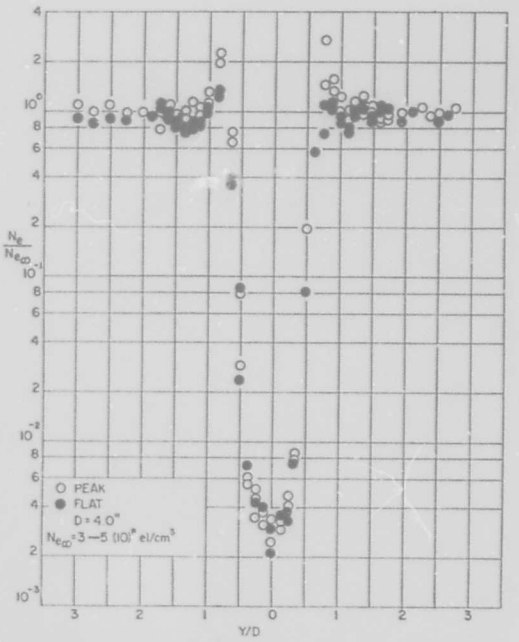

Fig. 10. Nondimensional electron density distribution in the wake of a 10° half angle cone at 0° angle of attack at $x/d = 0.25$.

In Fig. 11, a normalized plot of the electron density, as obtained in this work at a station $x/D = 3$ in the wake, is compared with the normalized density at the same station obtained (*Munz and Zempel*, 1963) through the use of an electron beam. The good qualitative agreement of the two techniques not only supplement each other but establishes the electrostatic probe technique as a very simple and powerful tool in field tracing. A composite of electron density profiles obtained by this method at several stations in the wake of the cone at 0° angle of attack is shown in Fig. 12. The composite data obtained behind the same 10° half angle cone at 10° angle of attack is shown in Fig. 13. In Fig. 14, a comparison of the profiles at two different axial stations in the wake of a 10° half angle cone at 0° and 10° angles of attack is shown. A definite displacement of the symmetry line of the profile from the centerline can be observed. As can be seen in Figs. 12 and 13, there is an overshoot in the electron density at the outer edges of the wake,

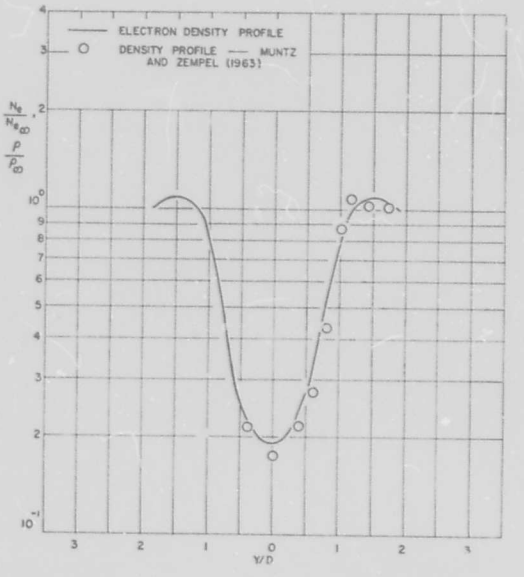

Fig. 11. Comparison of electron and neutral density profiles for $x/D = 3.0$.

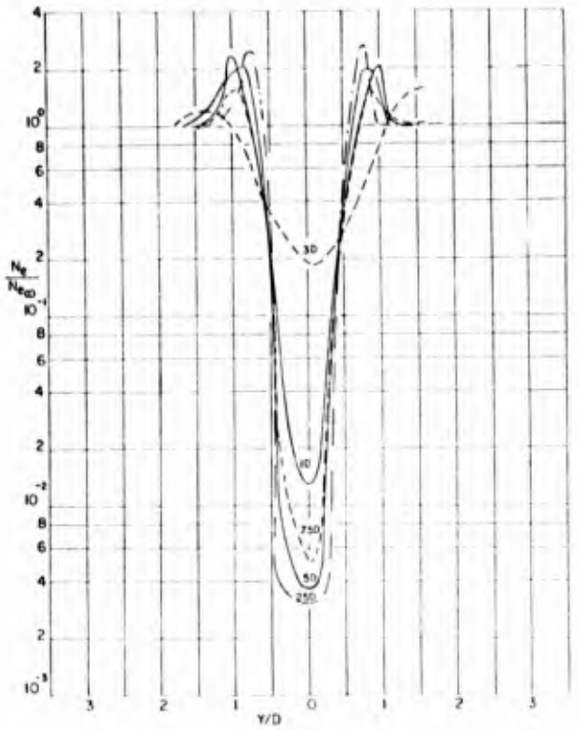

Fig. 12. Composite of radial profiles in the near wake of a 10° half angle cone at various axial stations at 0° angle of attack.

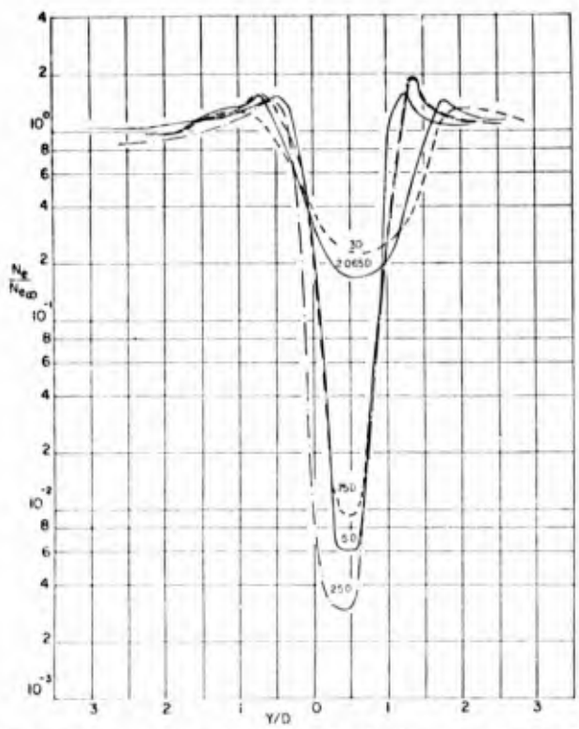

Fig. 13. Composite of radial profiles in the near wake of a 10° half angle cone at various axial stations at 10° angle of attack.

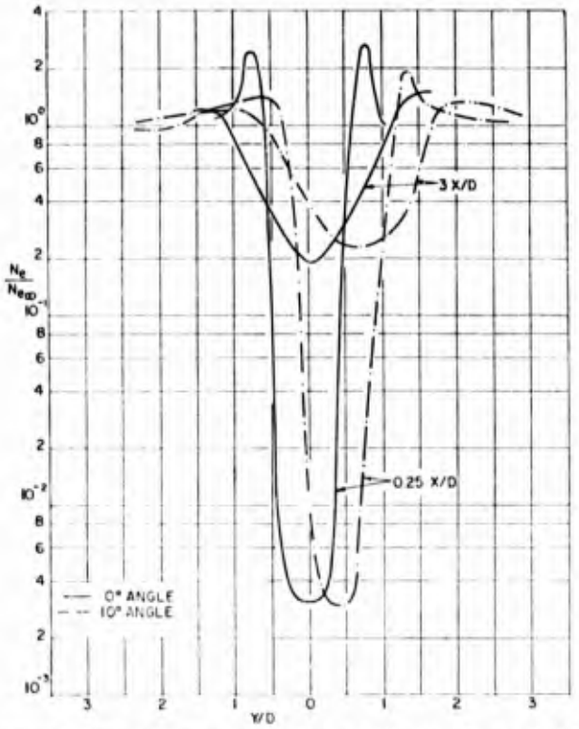

Fig. 14. Composite of the radial density distribution in the wake of a 10° half angle cone at 0° and 10° angle of attack.

which is decreasing in amplitude and increasing in distance from the axis of the wake, as the rake distance from the model is increasing. This overshoot is indicative of the shock location. Figure 15, reproduced

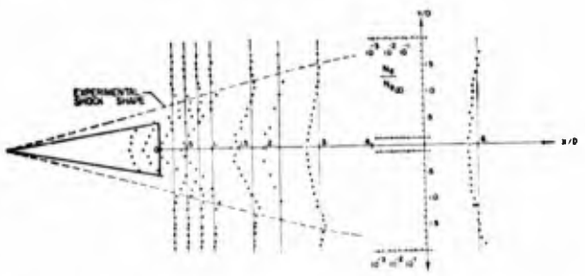

Fig. 15. Experimental representation of the flow field of the 10° half angle cone at 0° angle of attack.

from earlier work (*Lederman* et al., 1969*b*), indicates this explicitly, and provides a method of obtaining the shock location in the near wake utilizing electrostatic probes. This method was used subsequently to obtain the shock shape in the wake behind the cone at 10° angle of attack and the blunted cones of bluntness ratio 0.33 and 0.66. The shock shapes are shown in Figs. 16, 17, 18, and 19.

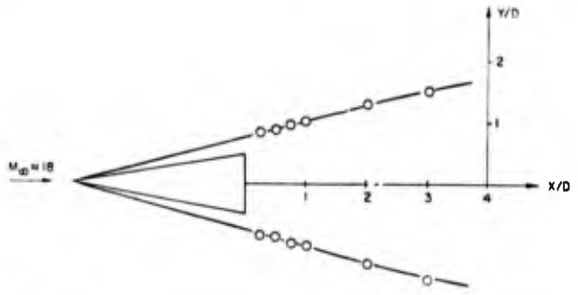

Fig. 16. Experimental shock shape for a 10° half angle cone at 0° angle of attack.

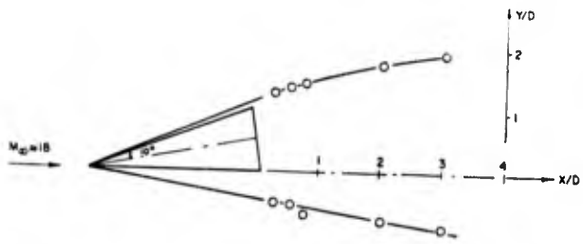

Fig. 17. Experimental shock shape for a 10° half angle cone at 10° angle of attack.

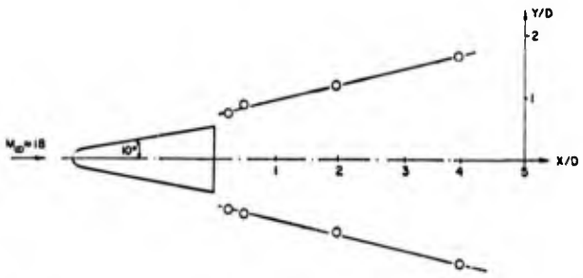

Fig. 18. Experimental shock shape for a 10° half angle blunted cone ($B = 0.333$) at 0° angle of attack.

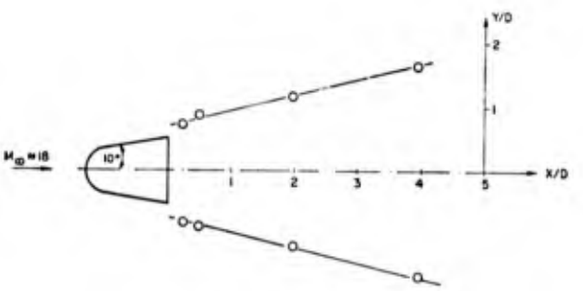

Fig. 19. Experimental shock shape for a 10° half angle blunted cone ($B = 0.666$) at 0° angle of attack.

Using the same technique the wake of an Apollo Command Module model was tested. Figure 20 presents a typical normalized electron density distribution profile at an axial distance from the rear tip of the model of $x/D = 0.25$. The shock shape in the wake of the model is shown in Fig. 21. The data thus obtained are compared with the data in Kruse (1968). The agreement is quite good, giving further support to the electrostatic probe method.

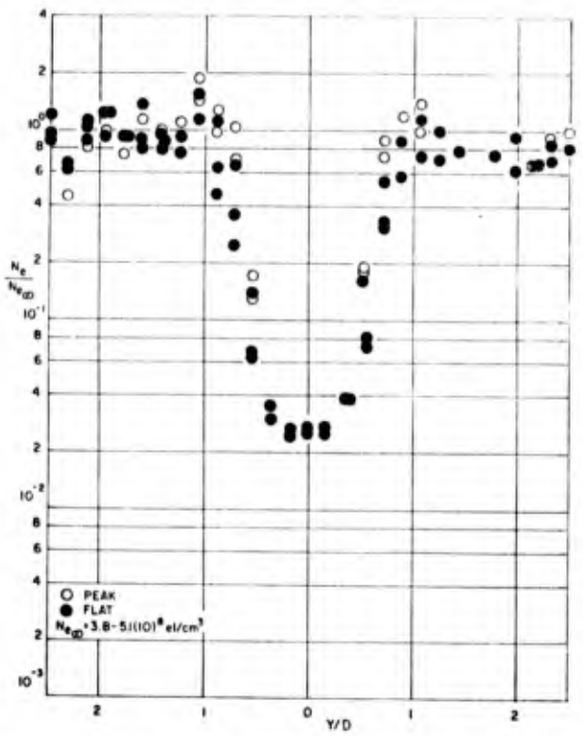

Fig. 20. Nondimensional electron density distribution in the near wake of the Apollo Command Module at $x/D = 0.25$.

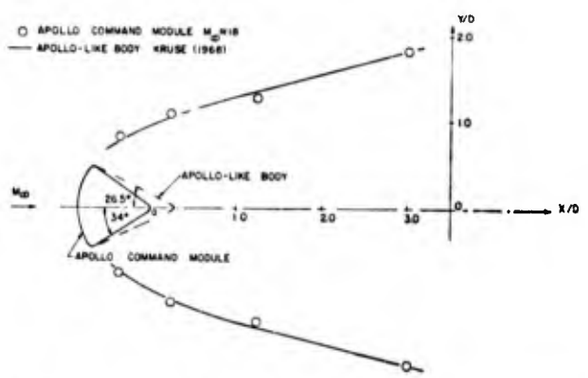

Fig. 21. Experimental shock shape for the Apollo Command Module at 0° angle of attack.

Finally, in Fig. 22, a photographic view is shown of the Apollo Command Module model during a test, taken by the luminosity developed in the stagnation region as a result of ionization and recombination occuring there.

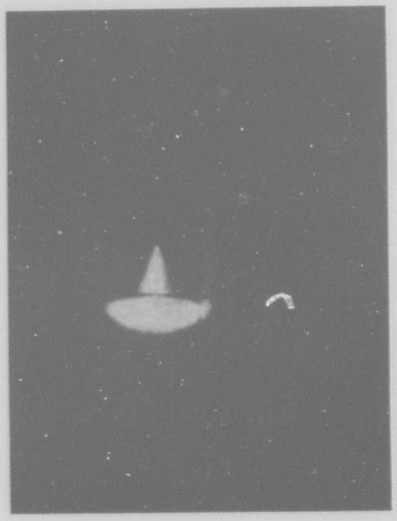

Fig. 22. Photograph of the luminous front of the Apollo Command Module during a test.

VI. DISCUSSION OF RESULTS AND CONCLUSIONS

As is clearly evident from the experimental results obtained, and in particular the results presented in Figs. 1 and 8, the formal extension of the formulation of Eq. (1) into the transitional and continuum regime follow the same empirical curve as the extension into the regime of $r_p/\lambda_D<3$ In the free molecular collisionless regime. The deviation of the experimentally determined α_p in the transitional and continuum regime from the free-molecular collisionless values determined by Laframboise is very much in evidence. As has been noted previously, the condition imposed by the Lafranmboise solutio of $r_p/\lambda_D>3$ is satisfied in this regime; however, the free-molecular conditions are not. This is evident from an inspection of Table I, where the mean free paths are tabulated. As the test station is moved upstream in the nozzle, the flow changes from free-molecular through transitional to continuum with respect to some probes, at least as far as the neutral-neutral and ion-neutral mean free paths are concerned. The deviation from the free-molecular collisionless theory of Laframboise was therefore to be expected. The results of Fig. 8, in conjunction with the data of Fig. 7, reaffirms the validity of the Laframboise theory in the interval where all the conditions of this theory are met. They also provide the necessary values of the nondimensional current α_p to enable the experimentalist to obtain easily the electron number densities from the collected current densities. It should be noted here that the dependence of the current collection vs. the *l/d* ratio remained unaffected by the change in the regime of probe operation. It remained essentially the same as for the free-molecular collisionless regime shown in Fig. 2. In reducing the collected current to its corresponding ion number density, this effect must be taken under account. At this point no attempt is being made here to explain, through a theoretical analysis, this behavior of the cylindrical probes, although some work along this line is being pursued in this and other laboratories. The experimental results, as presented in Figs 1, 2, and 8, are more than adequate to permit the application of the cylindrical electrostatic probe to flow field diagnostsics in most regimes encountered in many simulation facilities and actual reentry. Caution should, however, be exercised in the interpretation of the data. In chemically frozen flow fields, the electron density measured can be interpreted in terms of the neutral densities, provided diffusion is negligible. In chemically active flows no such correspondence can be established. As mentioned previously, the data obtained in this work and in particular the data presented in Fig. 11, where the electron density is compared with the neutral density obtained by means of an electron beam technique and the data of Fig. 21, where

TABLE I

MEAN FREE PATHS

x cm	λ_{n-n} cm x10^{-2}	λ_{n-i} cm x10^{+4}	λ_{i-n} cm x10^{-2}	λ_{e-n} cm	λ_{e-i} cm x10^{+1}	λ_{e-e} cm	λ_{i-e} cm x10^{-3}	λ_{i-i} cm
105	2.11	2.5	2.11	1.83	1.56	5.52	1.18	1.78
130	3.45	6.1	3.45	4.54	5.38	19.0	3.44	5.20
170	7.03	8.2	7.03	9.25	7.13	25.20	3.94	5.95
260	19.60	36.2	19.60	25.80	27.0	95.5	12.40	18.70
440	60.00	120.0	60.00	78.80	93.0	330.0	33.50	50.4

the shock shape obtained from the electrostatic probes is compared with the shock shape obtained by optical means, confirms the applicability of the probes to flow field diagnostics. It must, however, be remarked that in both cases the ambient neutral density was orders of magnitude higher than in the work reported here, which would have made the other techniques useless or at best, very difficult to apply. The composites of the flow field behind the cone at 0° and 10° angles of attack demonstrates the details with which a flow field can be obtained by applying this method. The sensitivity of this method to flow field perturbation is also demonstrated by Fig. 14, in which a comparison is made between the profiles at 0° and 10° angles of attack. The determination of the shock shapes presents some problems under the diffused shock conditions encountered in this investigation. This was found to be particularly difficult at large distances from the base of the models where the electron density approaches the free stream density. It should, however, be pointed out again that besides the fluorescent technique this is probably the only and simplest technique to obtain the shock shape under those low density conditions.

In concluson, it can be stated that the extension, of the range of applicability of the electrostatic porbe into the transitional and continuum regime provides the experimentalist with a simple and powerful tool in flow field diagnostics. The only necessary precondition for the use of this technique in flow field diagnostics is the presence of ionized particles.

ACKNOWLEDGEMENTS

This research has been conducted in part under Contract Nonr 839(38) for Project Strategic Technology supported by the Advanced Research Project Agency under Order No. 529 through the Office of Naval Research; and in part under Contract DAHCO4–69–C–0077, monitored by the U.S. Army Research Office and supported by the Advanced Research Projects Agency under ARPA Order No. 1442.

REFERENCES

ALLEN, G. E., R. L. F. BOYD AND P. REYNOLDS, 1957. Collection of positive ions by a probe immersed in a plasma, *Proc. Phys. Soc.*, **70**, 297.

BERNSTEIN, I. B. AND I. N. RABINOWITZ, 1959. Theory of electrostatic probes in low density plasmas, *Phys. Fluids*, **2**, 112.

BLOOM, M. H. AND S. LEDERMAN, 1967, Measurement of the Ionized Flow in a Shock Tunnel by Means of Resonant Cavities and Electrostatic Probes, Polytechnic Institute of Brooklyn, PIBAL Rept. No. 1019.

GRAF, K. A., 1965. The Determination of Spacially Non-uniform Electron Density Distribution, University of Toronto, UTIAS Rept. No. 108, AFOSR 65-0935.

HEALD, M. A. AND C. B. WHARTON, *Plasma Diagnostics with Microwaves*. J. Wiley & Sons, New York.

KRUSE, R. L., 1968. Transition and Flow Reattachment Behind an Apollo Like Body and Mach Numbers to 9, NASA TN D-4645.

LAFRAMBOISE, Y. G., 1966. Theory of Spherical and Cylindrical Langmuir Probes in a Collisionless Maxwellian Plasma at Rest, University of Toronto, UTIAS Rept. No. 108.

LANGMUIR, I. AND H. M. MOTT-SMITH, 1926. Theory of collectors in gaseous discharges, *Phys. Rev.*, **28**, 727.

LEDERMAN, S., M. ABELE AND M. VISICH, JR., 1964. Microwave Techniquees Applicable to Shock Tube Measurements, Polytechnic Institute of Brooklyn, PIBAL Rept. No. 857.

LEDERMAN, S., D. S. WILSON AND E. F. DAWSON, 1967. Langmuir probe and microwave technique for ionized flow. *IEEE Trans. on Aerospace and Electronic Systems*, AES-3.

LEDERMAN, S., M. H. BLOOM AND G. F. WIDHOPF, 1968. Experiments on cylindrical electrostatic probes in a slightly ionized hypersonic flow, *AIAA J.*, **6**, 2133-2139.

LEDERMAN, S., M. H. BLOOM AND G. F. WIDHOPF, 1969*a*. Field tracing with electrostatic probes in low density slightly ionized flows, '69 ICIASF Record, 43–50.

LEDERMAN, S., M. H. BLOOM AND G. F. WIDHOPF, 1969*b*. Laboratory measurements of electron-density distributions in the near wake, *AIAA J.*, **7**, 1421–1429.

LEEUW, J. H., DE, 1963. Electrostatic plasma probes, *Fifth Biennial Gas Dynamics Symposium.*

MURZ, E. P. AND R. E. ZEMPEL, 1963. Slender Body Near Wake Density Measurements at Mach Numbers 13 and 18, General Electric Co., Rept. No. 63SD718.

SONIN, A. A., 1966. Free-molecule Langmuir probe and its use in flow field studies, *AIAA J.*, **4**, 1588.

SU, C. H. AND S. H. LAM, 1963. Continuum theory of spherical electrostatic probes, *Phys. Fluids*, **6**, 1479.

VISICH, M., JR., S. LEDERMAN AND W. H. MAK, 1965. The Combustion Driven Shock Tunnel of the Polytechnic Institute of Brooklyn, PIBAL Rept. No. 847.